ADVANCES IN ATMOSPHERIC SCIENCES, VOL. 21, NO. 6, 2004, 964–975

A Modeling Study of the Effects of Anomalous Snow Cover over the Tibetan Plateau upon the South Asian Summer Monsoon

LIU Huaqiang*[1] (刘华强), SUN Zhaobo[2] (孙照渤), WANG Ju[2] (王 举), and MIN Jinzhong[1] (闵锦忠)

[1] *Key Laboratory for Meteorological Disasters and Environmental Change, Nanjing Institute of Meteorology, Nanjing* 210044

[2] *Department of Atmospheric Sciences, Nanjing Institute of Meteorology, Nanjing* 210044

(Received 3 September 2003; revised 22 April 2004)

ABSTRACT

The effect of anomalous snow cover over the Tibetan Plateau upon the South Asian summer monsoon is investigated by numerical simulations using the NCAR regional climate model (RegCM2) into which gravity wave drag has been introduced. The simulations adopt relatively realistic snow mass forcings based on Scanning Multi-channel Microwave Radiometer (SMMR) pentad snow depth data. The physical mechanism and spatial structure of the sensitivity of the South Asian early summer monsoon to snow cover anomaly over the Tibetan Plateau are revealed. The main results are summarized as follows. The heavier than normal snow cover over the Plateau can obviously reduce the shortwave radiation absorbed by surface through the albedo effect, which is compensated by weaker upward sensible heat flux associated with colder surface temperature, whereas the effects of snow melting and evaporation are relatively smaller. The anomalies of surface heat fluxes can last until June and become unobvious in July. The decrease of the Plateau surface temperature caused by heavier snow cover reaches its maximum value from late April to early May. The atmospheric cooling in the mid-upper troposphere over the Plateau and its surrounding areas is most obvious in May and can keep a fairly strong intensity in June. In contrast, there is warming to the south of the Plateau in the mid-lower troposphere from April to June with a maximum value in May. The heavier snow cover over the Plateau can reduce the intensity of the South Asian summer monsoon and rainfall to some extent, but this influence is only obvious in early summer and almost disappears in later stages.

Key words: snow cover, Tibetan Plateau, South Asian monsoon, numerical simulation

1. Introduction

Many studies have demonstrated that the interannual variability of the Asian summer monsoon is significant and the reasons for the variability are very complex. The anomaly of Eurasian snow cover during the preceding winter/spring has been proposed as one of the affecting factors. Some observational studies suggest an inverse relation between the Eurasian winter and spring snow accumulation and the subsequent summer monsoon rainfall over India (Hahn and Shukla, 1976; Dickson, 1984). Parthasarathy and Yang (1995) further confirmed this relation with additional data. Shukla (1987) hypothesized that an excessive snowfall during the previous winter and spring seasons can delay the build-up of the monsoonal temperature gradient because part of the solar energy will be reflected and part will be utilized for melting the snow or for evaporating the soil moisture. Some of the resulting meltwater is stored in the form of soil moisture, and this water continues to inhibit the surface sensible heating through the increase of the latent heat of vaporization. A relatively smaller amount of energy will be left for warming the surface and the atmosphere. These physical mechanisms responsible for the relation between Eurasian snow cover and the Asian summer monsoon have been tested in many general circulation model (GCM) studies (Yeh et al. 1983; Barnett et al. 1989; Yasunari et al. 1991).

The significance of the Tibetan Plateau as an elevated heat source for the onset of the Asian summer monsoon has been discussed by many authors (e.g.,

*E-mail: hqliu160@sohu.com

Hahn and Manabe, 1975; Wu and Zhang, 1998). It is hypothesized that the Tibetan Plateau snow mass influences the strength of the Asian summer monsoon by delaying the time when significant surface sensible heating occurs and by constraining the amount of available heating. Zwiers (1993) found a positive correlation between Tibetan sensible heat flux and southeast Asian rainfall, suggesting an inverse relationship between Tibetan snow cover and southeast Asian rainfall, and pointed out that it was the Tibetan snow cover rather than the Eurasian snow cover that influenced the monsoon circulation. Also, Ose (1996) compared the atmospheric response to the regional snow mass anomalies in early spring over Tibet, Eastern Europe, and Siberia by ensemble GCM experiments. He found that the positive snow mass anomalies over Tibet produced the largest cooling anomalies in the atmosphere from spring to early summer, and almost no significant forcing anomalies were systematically formed by the snow mass anomalies over Eastern Europe and Siberia. Vernekar et al. (1995) found that energy used in melting excessive snow reduced the mid-tropospheric temperature over the Tibetan Plateau. The result was to reduce the mid-tropospheric meridional temperature gradient over the Indo-China Peninsula, which weakened the monsoon circulation. However, with correlation analysis, Li (1995) considered that there was no apparent relationship between the High Asian snow cover in the preceding winter and Indian monsoon rainfall in the following summer.

In China, there has been a long history of studies of the possible relationship between the snow cover over the Tibetan Plateau during previous winter and spring seasons and subsequent precipitation in flood periods of eastern China. These works include diagnostic analyses (e.g., Chen and Yan, 1978; Guo and Wang, 1986; Wu and Qian, 2000; Chen, 2001) and numerical simulations (e.g., Lu and Luo, 1994; Zhang and Tao, 2001; Qian et al. 1999). However, many of these studies lay particular stress on the effects of anomalous snow cover over the Tibetan Plateau upon the East Asian summer monsoon and summer rainfall over the eastern China.

Up to now, almost all of the numerical simulations were based on GCMs with low horizontal resolution. These models were able to simulate large-scale features of the Asian monsoon but they were deficient in simulating the regional atmospheric responses to the Tibetan Plateau snow cover anomaly. Meanwhile, the results in recent numerical simulations of Asian summer monsoon climate differed notably due to the different spatial scales and snow depth anomalies given in each model. In particular, many experiments adopted the "Bucket Model" to simulate the land surface process and it was shown that the land surface scheme did not store meltwater effectively. Consequently, the effect of the snowpack variations might have been reduced to that of the corresponding albedo variation alone. Sometimes, the snow forcing in the model was unreasonable. It is therefore suggested that the physical mechanism relating the Tibetan Plateau snow cover with the Asian monsoon might not be properly simulated in the model.

There are two questions that should be answered. Which stage of the South Asian summer monsoon can be affected by anomalous snow cover over the Tibetan Plateau during the previous winter/spring season, whole summer, or only early summer? What are the physical mechanism and spatial characteristics for this influence? The purpose of the present study is to investigate the connection of the snow cover anomaly over the Tibetan Plateau and the South Asian summer monsoon with the aid of a regional climate model (RCM). The regional climate model has a relatively higher resolution and is able to simulate the main regional response of the South Asian summer monsoon to snow cover over the Tibetan Plateau. The model should have a relatively perfect description for land surface processes, and a relatively realistic Tibetan snow mass forcing will be used in the experiments. It is expected that the physical mechanism and spatial structure for the sensitivity of the South Asian summer monsoon to the snow cover anomaly over the Tibetan Plateau can be revealed by numerical simulation with a regional climate model. Section 2 describes the experimental design. The results are presented in section 3. A discussion and concluding remarks are given in section 4.

2. Description of the model and experiment design

The NCAR regional climate model RegCM2 (Giorgi et al., 1993) is used for the present experiments. The model's surface physics calculations are performed using the Biosphere-Atmosphere Transfer Scheme (BATS) version BATS-1E (Dickinson et al. 1993). The snow sub-model in BATS-1E assumes the snow cover as a one-layer system with a time-dependent snow depth, snow density, and snow albedo for 15 types of vegetation. At every time step, the snow aging and the fraction of the grid square covered by snow are calculated, from which the thermal conductivity and volumetric specific heat of snow and the composite soil/snow layer are derived. The composite soil/snow temperature is computed using the force-restore method.

Liu and Qian (2001) introduced the gravity wave drag induced by subgrid-scale orography to RegCM2 which is used in present study. The model vertical structure includes 15 unequally-spaced σ levels with the model top at 10 hPa. The σ values are 0.0, 0.04, 0.1, 0.17, 0.25, 0.35, 0.46, 0.56, 0.67, 0.77, 0.86, 0.93, 0.97,0.99 and 1.0. In the simulations, the Blackadar high resolution PBL parameterization and Anthes-Kuo cumulus parameterization are selected. The time splitting scheme is applied to the model integration.

The model domain is 5600×4320 km^2 in size with a horizontal resolution of 80 km, it encompasses the Tibetan Plateau and South Asia with a maximum topography height of 5500 m, and its center is located at (26.5°N, 75°E). The meteorological initial and lateral boundary conditions necessary to drive the model runs are interpolated from a monthly mean climatology based on 40-yr NCEP/NCAR (National Centers for Environmental Prediction/National Centre for Atmospheric Research) reanalyses data (1958–1997). A sponge lateral boundary is adopted and the size of the buffer zone is 5 boundary cycles. The model is integrated under a climatic state for a period from 15 February to 31 July. The vegetation cover is prescribed from the climatology. The initial soil moisture content depends on the specified vegetation type through the use of a soil water availability function. Time-dependent sea surface temperatures are interpolated from a set of climatic monthly SST grid data. The time step length for the model integration is 180s.

To prescribe the initial snow cover over the Tibetan Plateau, we need a measure of the geographical distribution of snow depth. The only available global dataset of snow depth is from the Nimbus-7 Scanning Multi-channel Microwave Radiometer (SMMR) during the period of 1979 to 1987. The initial snow cover is prescribed from the February climatology based on nine years of data. Estimated by the observational data, the snow mass forcing in the model can be considered reasonable. The distribution of initial snow depth over the Tibetan Plateau for the control experiment is shown in Fig. 1. It can been seen that there are two main snow cover areas which are located in the eastern part and western part of the Tibetan Plateau respectively, and the central part of the Plateau has less snow mass.

In the BATS scheme, the snow water equivalent on the ground is updated from

$$\frac{\partial S}{\partial t} = P_{\rm s}(1 - A_{\rm v}) - F_{\rm q} - S_{\rm m} + D_{\rm s}\ , \qquad (1)$$

where S is snow mass (kg m^{-2}) or is measured in terms of liquid water content (mm), $P_{\rm s}$ is snowfall rate (kg m^{-2} s^{-1}), $A_{\rm v}$ is the fraction of grid square covered by vegetation, $D_{\rm s}$ is the corresponding rate at which excess snow falls from the leaves (kg m^{-2} s^{-1}), $S_{\rm m}$ is snowmelt rate, and $F_{\rm q}$ is the rate of sublimation (kg m^{-2} s^{-1}).

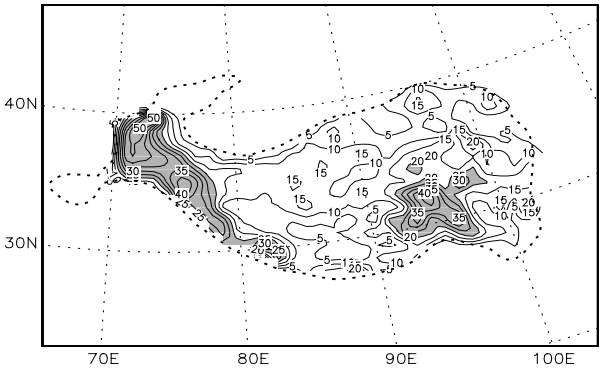

Fig. 1. Initial snow depth distribution over the Tibetan Plateau in the control experiment (Units: cm).

Two snow mass experiments are designed besides the control experiment (denoted by CON): the heavy snow experiment (HSE) and the light snow experiment (LSE). In the HSE and LSE experiments, the initial snow depth over the Tibetan Plateau is increased by 50% and decreased by 50% compared with the CON experiment respectively. Correspondingly, the snowfall rate given by the model's condensation scheme is increased by 50% in HSE and decreased by 50% in LSE without implications for the atmospheric heat and moisture balance at the time it falls. Therefore a larger (smaller) amount of snow in HSE (LSE) is available for melting and evaporation processes at the later stages of the simulation. We applied the altered snowfall rate only to the region of the Tibetan Plateau. There is no difference in the initial area extent of snow cover over the Plateau between these experiments. Over the Tibetan Plateau, the variance in snow depth or snow volume is more significant than that in snow coverage (Li, 1995). The intensity of snow mass anomalies selected in the present study are basically in keeping with the realistic inter-annual variability of total snow cover over the Tibetan Plateau from SMMR snow depth data as shown by Li (1996).

In the present study, the initial snow depth is increased (decreased) in the HSE (LSE) experiment by an identical rate of 50% over the whole Tibetan Plateau. But the inter-annual variability of snow cover over the Tibetan Plateau is not regionally homogeneous. For example, by using SSM/I derived snow depth data, Yasunari et al. (2000) found that the inter-annual variation of winter snow cover distribution over the Tibetan Plateau shows a remarkable east-

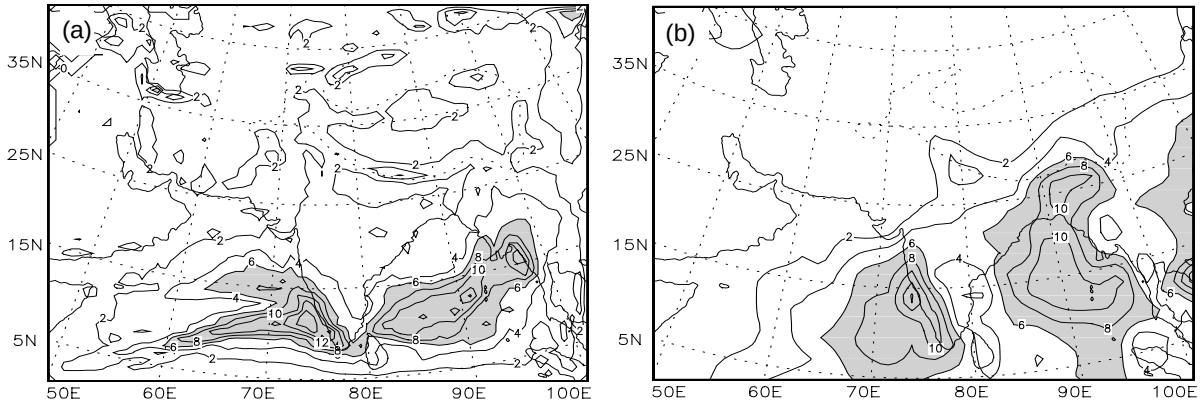

Fig. 2. (a) CON and (b) NCEP/NCAR reanalyses derived rainfall rates in June. Units: mm d^{-1}.

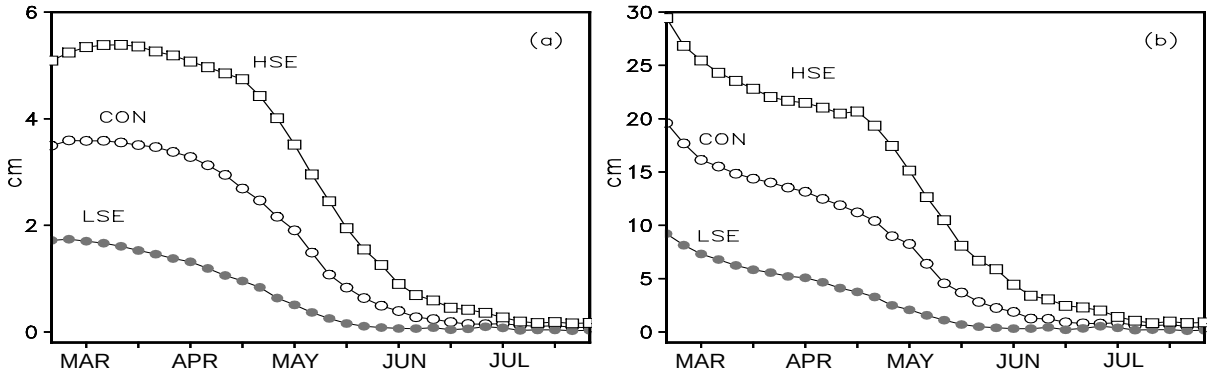

Fig. 3. Simulated seasonal variation of snow cover averaged over the Plateau. (a) Snow water equivalent. (b) Snow depth. Units: cm. Tick marks on the abscissa refer to the beginning of the month.

west dipole-like pattern, i.e., when the snow covers widely over the eastern (western) part of the Plateau, the snow cover over the western (eastern) part is less than normal. The effects of anomalous snow cover over the western and eastern parts of Tibetan Plateau will be compared in future studies. This paper only discusses the effects of the integrated snow cover anomaly over the Tibetan Plateau.

3. Simulation results

3.1 *Control run*

The precipitation is an important factor in the summer monsoon circulation. Figure 2a presents the pattern of the CON-given precipitation rate in June. Figure 2b shows the pattern of the climatological rainfall rate from NCEP/NCAR reanalyses in June. The simulated rainfall pattern basically resembles the climatological rainfall pattern over the India region, i.e., a large center of maximum rainfall in the Bay of Bengal and a relatively smaller maximum on the west coast of India. The South Asian monsoon rainfall in June is generally reproduced with correct locations.

3.2 *Simulated seasonal variation of total snow mass over the Plateau*

For the modeling study on the influence of snow forcing, it is very important that the simulated seasonal variation of snow cover be close to reality. Because of the special geographical position and terrain height, it is more difficult to accurately simulate the snow cover over the Tibetan Plateau. Some studies have demonstrated that the BATS scheme generally overestimates surface snow mass (e.g., Yang et al., 1997; Sun et al., 1999). Figures 3a and 3b show the seasonal variation of pentad-mean snow water equivalent and snow depth averaged over the Plateau (defined as the region with terrain height in excess of 2500 m), respectively. As seen in Fig. 3a, the initial snow mass in HSE (LSE) is almost 50% larger (smaller) than that in CON. In the HSE experiment, the snow mass slowly increases before mid-March. The difference (HSE–CON) and difference (LSE–CON) of snow mass reach their maximum values at mid-March and

gradually decrease in later stages. Most of the snow over the Plateau is melted by the end of June in the three experiments. Being different than snow water equivalent, the snow depth displays a rapidly decreasing trend in the beginning stages of the model run in the three experiments. This may be mainly due to the treatment of initial snow as new snow in BATS with a small density of 100 kg m^{-3}, so the snow density grows quickly due to snow compaction processes in the beginning stages of the simulations. Figures 3a and 3b indicate that the small snow melting speed over the Tibetan Plateau, maintains the spring additional snow mass, probably due to the Plateau's high elevation.

3.3 *Analysis of surface heating over the Tibetan Plateau*

The surface energy balance can be written as

$$F_{\mathrm{S}}^{\downarrow}(1-\alpha_{\mathrm{S}})+F_{\mathrm{LW}}^{\downarrow}=\varepsilon\sigma T_{\mathrm{S}}^{4}+F_{\mathrm{SH}}^{\uparrow}+F_{\mathrm{LH}}^{\uparrow}+F_{\mathrm{G}}^{\downarrow}+F_{\mathrm{M}}\,, \tag{2}$$

where

$F_{\mathrm{S}}^{\downarrow}$—solar radiation reaching the earth's surface

α_{S}—albedo of the earth's surface

ε—thermal emissivity of the earth's surface

σ—Stefan-Boltzman constant

$F_{\mathrm{LW}}^{\downarrow}$—atmospheric radiation arriving at the earth's surface

T_{S}—surface (ground) temperature

$F_{\mathrm{SH}}^{\uparrow}$—upward sensible heat flux

$F_{\mathrm{LH}}^{\uparrow}$—latent heat flux due to evaporarion of water (liquid to vapor)

$F_{\mathrm{G}}^{\downarrow}$—downward sensible heat flux to subsurface layers due to diffusion

F_{M}—latent heat energy used to melt snow (or ice). When snow is present on the ground, α_{S} is determined by BATS depending on the total fraction of the grid square covered by snow.

The five panels of Fig. 4 show the seasonal variation of the 10-d mean difference (HSE–LSE) of surface heat fluxes, snowmelt rate, percentage of snow coverage, surface temperature, and water storage of the

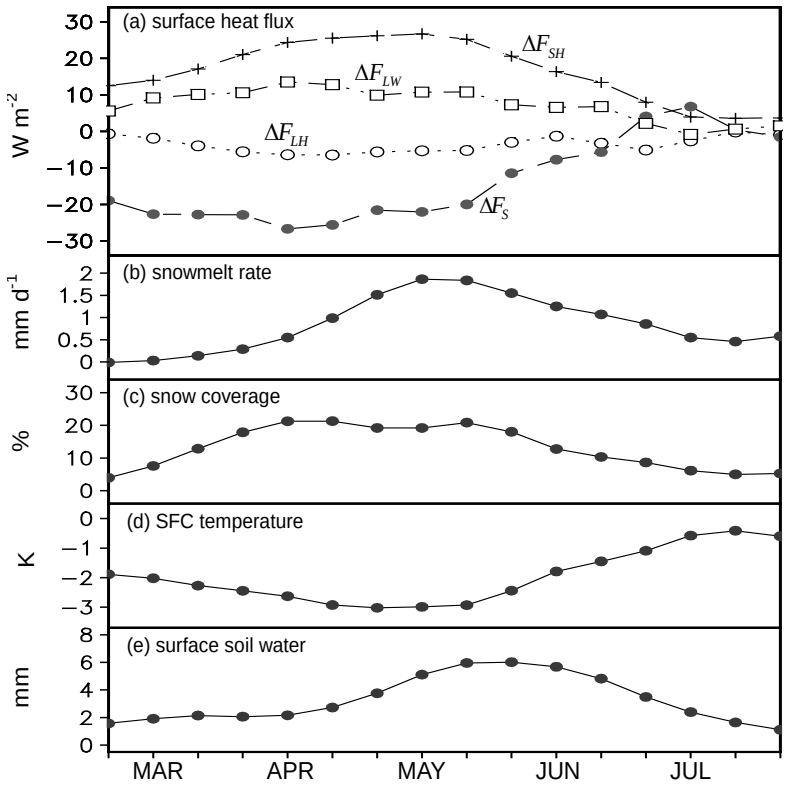

Fig. 4. Seasonal variation of difference (HSE—LSE) in surface heat fluxes (a), snowmelt rate (b), percentage of snow coverage (c), surface temperature (d), and water storage in the surface soil layer (e) area-weighted averaged over the Tibetan Plateau. Tick marks on the abscissa refer to the beginning of the month.

10-cm thick surface soil layer averaged over the Tibetan Plateau, respectively. Figure 4b shows there is no obvious difference in snowmelt rate over the Plateau before mid-March. The snowmelt rate is higher in HSE than in LSE with a maximum difference of about 1.5-mm water equivalent per day in early May. The difference in the percentage of snow coverage shown in Fig. 4c is positive with a maximum value of 20% from April to mid-May. The surface temperature difference (HSE–LSE) shown in Fig. 4d is negative from late February to June with a minimum of –3 K in late April and early May when the snowmelt difference is maximum. The negative surface temperature difference can last until the end of June but becomes unobvious in July. In Fig. 4a, $\Delta F_{\rm S}, \Delta F_{\rm LW}, \Delta F_{\rm SH}$, and $\Delta F_{\rm LH}$ represent the difference of net shortwave radiation, net longwave radiation, sensible heat flux, and latent heat flux absorbed by the surface, respectively. The positive (negative) values of the surface heat fluxes in Fig. 4a indicate that fluxes are converging (diverging) at (from) the surface to increase (decrease) the surface temperature in HSE. Prior to July, the contribution to surface temperature due to shortwave radiation absorbed and the latent heat flux due to evaporation are negative, whereas the differences of sensible heat flux and net longwave radiation emitted from the surface are positive. The shortwave radiation and the sensible heat flux are dominant. The difference in the shortwave radiation is less in HSE than in LSE. This is largely because of the snow albedo effect. The magnitude of the sensible heat flux difference is about the same as that of the shortwave radiation but of opposite sign; this indicates that the snow albedo effect in HSE is compensated by the sensible heat flux. When snow is present on the ground, the surface temperature is colder than without snow. The overlaying air over the colder surface is stable and hence the turbulence transfer process is less effective. Although snow is a good emitter of longwave radiation, the net longwave radiation is less in HSE than in LSE because of a lower surface temperature. The latent heat flux difference gradually increases as the snowmelt difference increases, which corresponds with the increasing of surface soil water storage as seen in Fig. 4e. Although the surface temperature is lower in HSE, the availability of snowmelt water dominates the evaporation.

In summary, the surface temperature over the Tibetan Plateau is colder in HSE than in LSE because of the snow albedo effect, the energy used in melting excessive snow, and that used in evaporating the soil moisture. The differences (HSE–LSE) of surface heat fluxes and surface temperature can last until June but almost disappear in July. According to the simulation results, the albedo effect is dominant, whereas the effects of snow melting and evaporation are relatively smaller. This is different than the results given by Barnett et al. (1989). They found that the effect of albedo alone was not significant but that the effect of snow melting and evaporation in addition to the albedo effect significantly diminished the intensity of Asian summer monsoon circulations. However, Yasunari et al. (1991) found that the albedo effect dominates in the spring to reduce the surface temperature, particularly over the Tibet.

3.4 *Atmospheric temperature fields*

To see the effects of excessive snow cover over the Tibetan Plateau upon atmospheric heating, we present the vertical cross sections of the atmospheric temperature difference (HSE–LSE) along 85°E from April to July in Fig. 5. We have seen from Fig. 4d that the surface temperature averaged over the Plateau is colder in HSE than in LSE from late February to June, and it is coldest in late April and early May. As seen in Fig. 5, there is obvious cooling above the Plateau surface from April to June, which reaches a maximum in May lagging behind the maximum cooling of the surface temperature to some extent. The atmospheric cooling is not restricted over the Plateau, for it takes a southward and northward expansion. So, over the Plateau and its sides, a south to north atmospheric cooling belt is formed in the mid-upper troposphere with the axis near 400 hPa. In contrast, there is warming to the south of the Plateau in the mid-lower troposphere from April to June with maximum values in May. Obviously, the atmospheric warming in the mid-lower troposphere balances the atmospheric cooling in the mid-upper troposphere under the limitation of static energy conservation. It should be pointed out that the atmospheric temperature difference (HSE–LSE) becomes much weaker in July; this indicates that the anomalous snow cover over the Tibetan Plateau has less effects on the atmospheric temperature after June.

3.5 *Geopotential height fields*

For geopotential height fields, we only give the monthly mean height difference in May. Figure 6 shows the vertical cross section of monthly mean height difference (HSE–LSE) along 85°E. It can be seen that there is a thin layer of positive height difference near the Plateau surface, above which is a thick layer of negative height difference with its horizontal axis near 200 hPa. This layer of negative height difference can last until June (figure omitted) and indicates that the excessive snow cover in HSE is unfavorable to

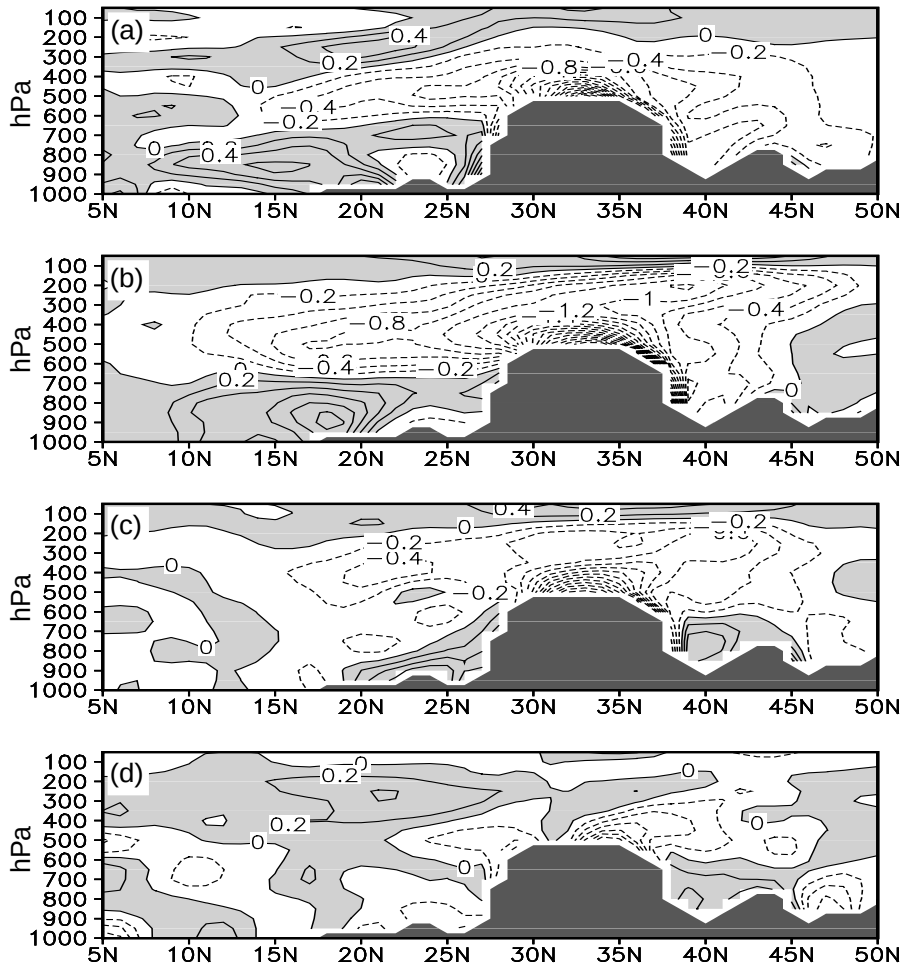

Fig. 5. Vertical cross section of monthly mean atmospheric temperature difference (HSE–LSE) along 85°E. Units: K. (a) April, (b) May, (c) June, (d) July.

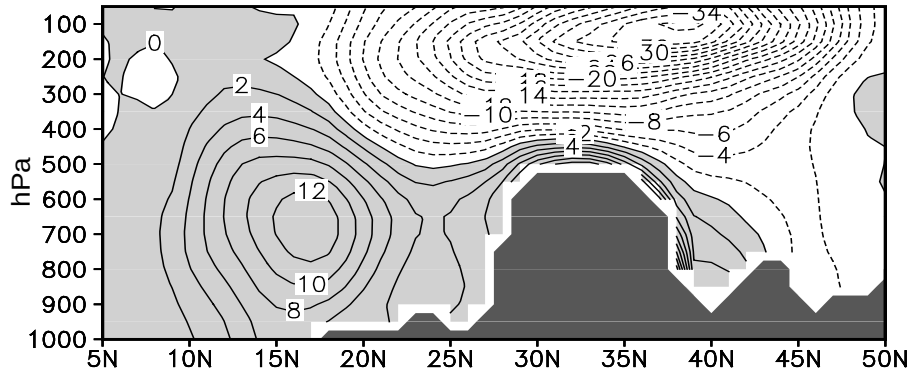

Fig. 6. Vertical cross section of monthly mean geopotential height difference (HSE–LSE) along 85°E in May. Units: gpm.

the development of the Tibetan High in early summer. Under this layer and to the south of the Plateau is a layer of positive height difference. The center of positive height difference is near 700 hPa. The strength of the negative height difference is obviously larger than that of the positive height difference. It can be concluded that heavier than normal snow cover over the Tibetan Plateau decreases the geopotential height over

the Plateau and its surrounding area in the upper troposphere, and increases the geopotential height in the lower troposphere to the south of the Plateau. This effect of anomalous snow cover over the Plateau upon geopotential height can last until late spring and early summer. The positive height difference is clearly related to the atmospheric warming to the south of the Plateau in mid-lower troposphere in May as shown in Fig. 5b.

Figure 7 illustrates the geopotential height difference (HSE–LSE) at 200 hPa from April to July. It can be seen that there are large areas of negative height differences at 200 hPa in April to June. The negative height differences are not just restricted to over the Plateau but cover more broad regions. This negative height difference is most obvious in May and can keep a certain intensity in June. The Tibetan High in the upper troposphere is an important member of South Asian summer monsoon system. Therefore the occurrence of the 200-hPa negative height difference (HSE–LSE) in June indicates that the excessive snow cover in HSE is unfavorable to the development of the Tibetan High in early summer. In July, the negative height difference becomes much weaker, suggesting that the anomalous snow cover over the Tibetan Plateau has less effects on the atmospheric geopotential height in the upper troposphere after June.

Figure 8 gives the patterns of geopotential height differences (HSE—LSE) at 700 hPa from April to July. It can be seen that the height differences (HSE—LSE) mainly occur to the south of the Plateau. For premonsoon circulation, as shown in Fig. 8b, the height differences are most obvious in May, and the geopotential height over South Asia is higher in HSE than in LSE. There are two centers of positive height differences (HSE—LSE) in May, one over the Bay of Bengal and the other located to the west of India. The climatological onset date of the summer monsoon at the southern tip of the Indo-China Peninsula is 1 June with a standard deviation of eight days (Soman and Kumar, 1993). However, some features of the monsoon circulation appear in May (Krishnamurti, 1985). One of the important features of the monsoon circulation is the establishment of the monsoon trough along the Ganges River from the northwest to the southeast. The intensity of the monsoon is proportional to the depth of the trough. The positive values of height difference over India in Fig. 8b indicate that the monsoon trough is relatively shallow in HSE.

In June, as seen in Fig. 8c, the HSE experiment gives a higher geopotential height over the Bay of Bengal and gives a lower height over western India. This also indicates that the monsoon trough is relatively shallower in HSE than in LSE in June. Fig. 8d shows that the height difference (HSE–LSE) is much weaker in July than in May or June, suggesting that the anomalous snow cover over the Tibetan Plateau has less effects on the atmospheric geopotential height in the lower troposphere after June.

3.6 *Wind fields*

Figure 9 shows the 700 hPa wind differences (HSE–LSE) from April to July. As is well known, another important feature of the monsoon circulation is that the lower tropospheric easterly flow over the Indian Ocean associated with the Mascarene High crosses the equator along the Somali Jet and then turns eastward to cross the Arabian Sea and the Indo-China Peninsula. The flow then continues northeastward along the monsoon trough. In May, the anomalous easterlies in Fig. 9b suggest that the westerlies over the southern part of the peninsula are weaker in HSE. In June, as seen in Fig. 9c, HSE also generally gives weaker westerlies between 5°–15°N in South Asia, especially weaker southwesterly flow over the Bay of Bengal. These results indicate that excessive snow cover over the Tibetan Plateau can weaken the Indian monsoon flow in the lower troposphere in early summer. However, as shown in Fig. 9d, the anomalous snow cover has less effects on the South Asian monsoon flows in July.

3.7 *Precipitation*

The precipitation differences between HSE and LSE from April to July are shown in Fig. 10. The difference in the rainfall pattern in Fig. 10b shows that the HSE experiment gives weaker rainfall in contrast with the LSE experiment in May over the Indo-China Peninsula and the Bay of Bengal. This is in agreement with the enhancement of anticyclonic circulations over these regions in HSE as mentioned above. In June, as shown in Fig. 10c, the HSE experiment also gives weaker rainfall over the Indo-China Peninsula and the northern part of the Bay of Bengal. This hints at an inverse relation between snow cover over the Tibetan Plateau and the South Asian monsoon rainfall in early summer. However, as seen in Fig. 10d, the rainfall difference (HSE–LSE) over South Asia in July is not obvious, suggesting that the anomalous snow cover over the Tibetan Plateau has less effects on South Asian monsoon rainfall after June.

4. Summary and concluding remarks

We have investigated the effect of anomalous snow cover over the Tibetan Plateau upon the South Asian summer monsoon by numerical simulations using the NCAR regional climate model (RegCM2). With high resolution and usage of BATS-1e in the model, the physical mechanisms responsible for the relationship between the snow cover over the Tibetan Plateau and the South Asian monsoon in early summer are revealed in more detail. Our main findings are:

(1) The heavier than normal snow cover over the Plateau can obviously reduce the shortwave radiation absorbed by the surface, which is compensated by the weaker upward sensible heat flux associated with cold-

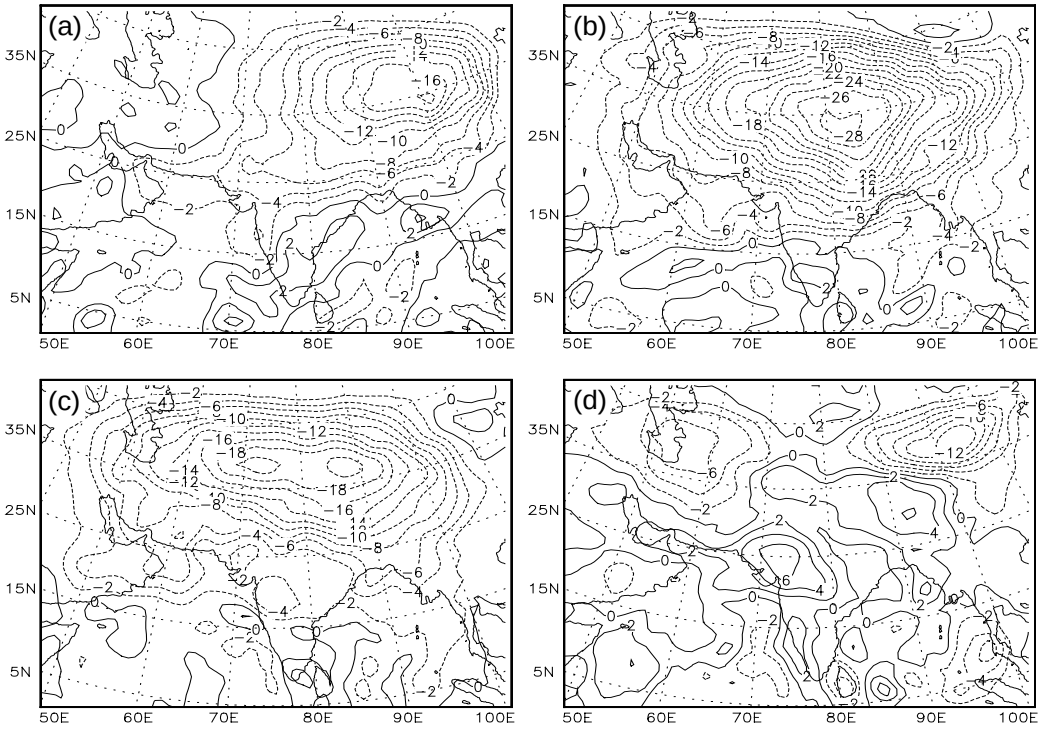

Fig. 7. Regional distribution of 200-hPa geopotential height difference (HSE–LSE). (a) April, (b) May, (c) June, (d) July. Units: gpm.

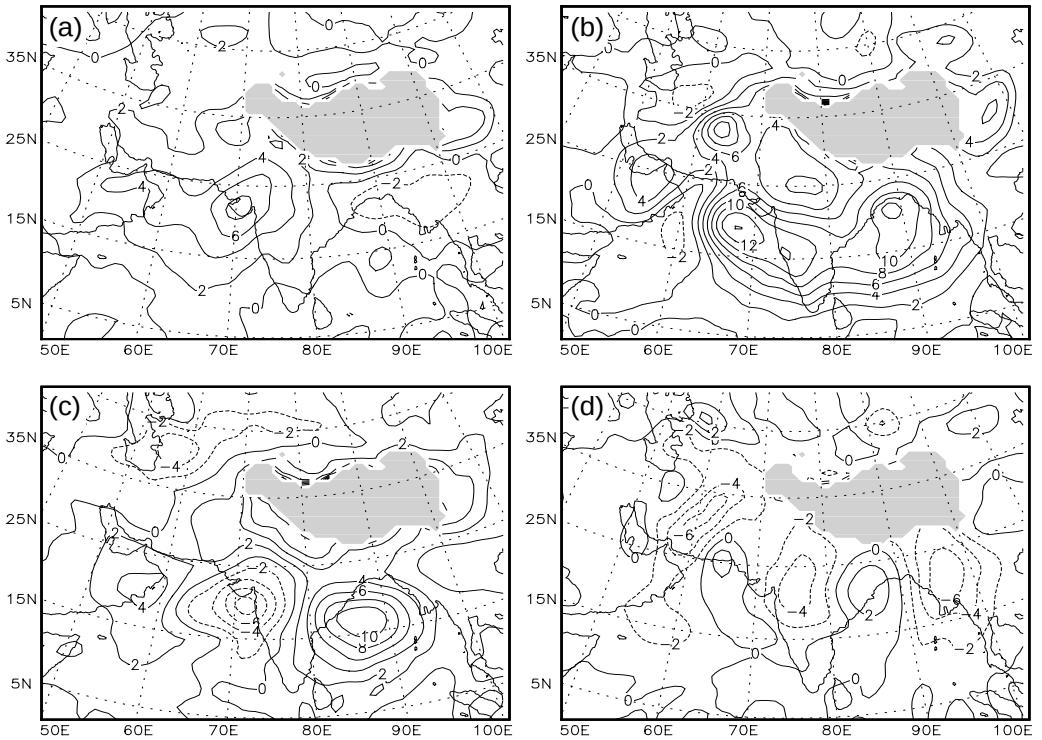

Fig. 8. Regional distribution of 700-hPa geopotential height difference (HSE–LSE). (a) April, (b) May, (c) June, (d) July. Units: gpm.

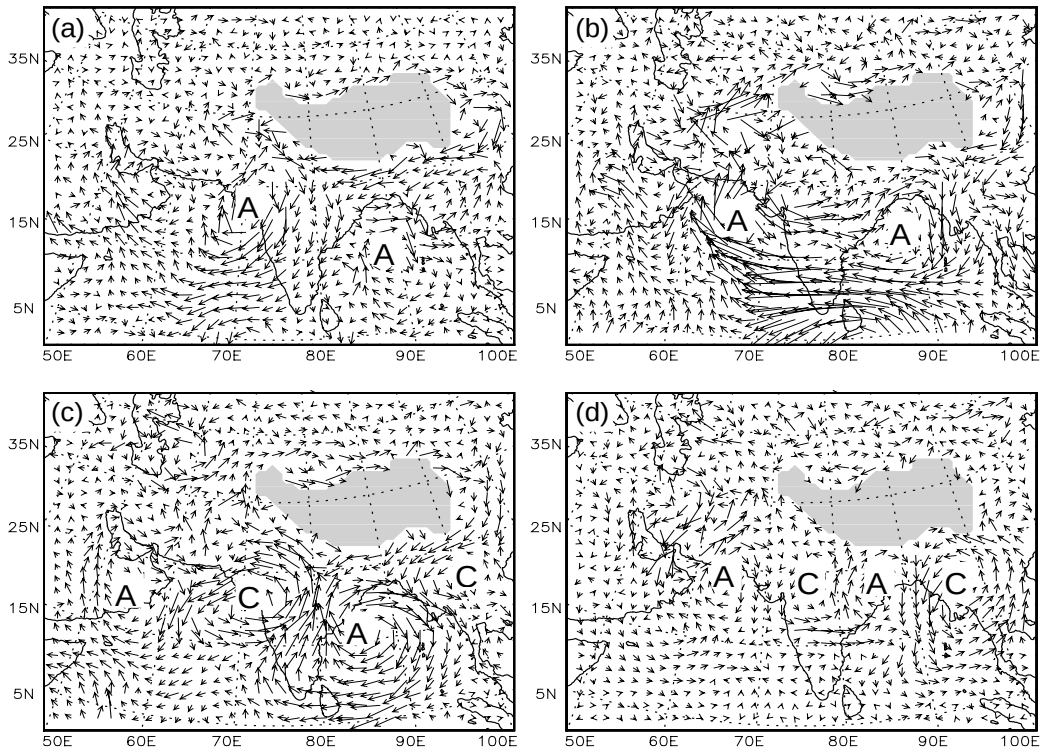

Fig. 9. Regional distribution of 700 hPa wind difference (HSE–LSE). (a) April, (b) May, (c) June, (d) July.

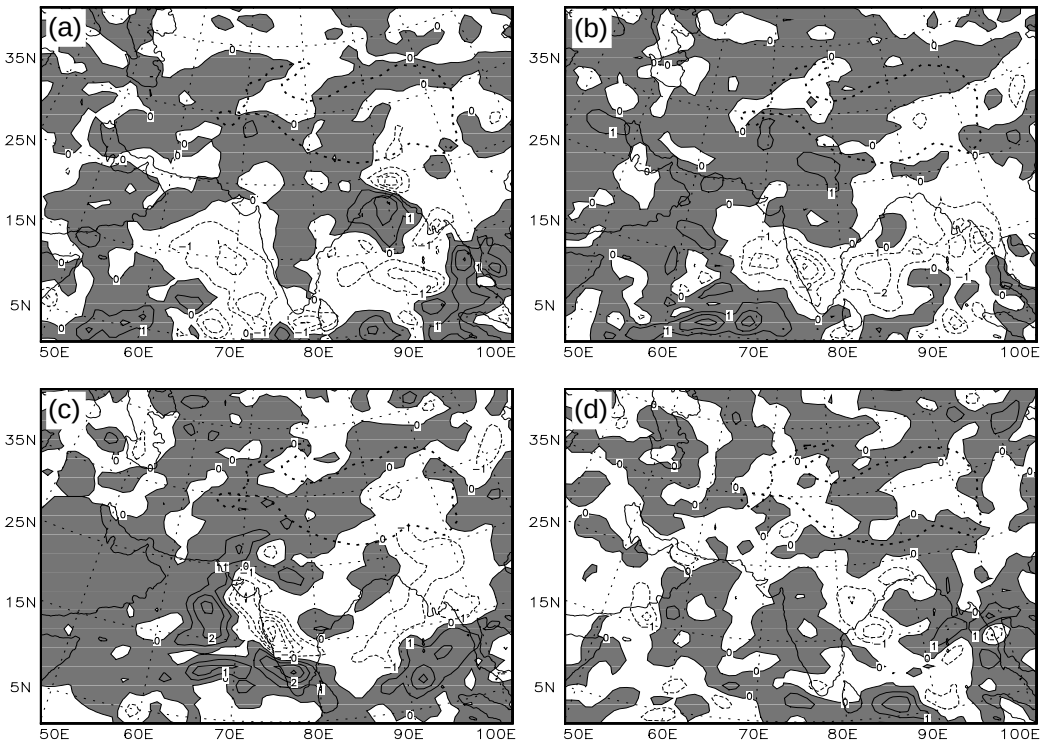

Fig. 10. Regional distribution of precipitation difference (HSE–LSE). (a) April, (b) May, (c) June, (d) July. Units: mm d^{-1}.

er surface temperature, whereas the variations of net longwave radiation and latent heat flux are relatively smaller. The anomalies of surface heat fluxes can last until June but become unobvious in July.

(2) The decrease of the Plateau surface temperature caused by excessive snow cover reaches its maximum value from late April to early May. The atmospheric cooling in the mid-upper troposphere over the Plateau and to its sides is most obvious in May and can keep a fairly strong intensity in June. In contrast, there is atmospheric warming to the south of the Plateau in the mid-lower troposphere. However, these responses of atmospheric temperature almost disappear in July.

(3) The heavier snow cover over the Plateau can reduce the intensity of the South Asian summer monsoon and the rainfall to some extent, but this influence is only obvious in early summer and not obvious in later stages.

We wish to conclude by pointing out some shortcomings of this paper: (1) The snow submodel in BATS-1e assumes the snow cover only as a one-layer system and does not distinguish the thermal regime of snow from that of soil. (2) The present BATS snow-rain criterion of 2.2°C is used in the model runs. Because the snow-rain temperature threshold may depend on the site elevation (in the mountains it may be higher) and on the geographical position, this constant of 2.2°C may not be appropriate for the snow cover process over the Tibetan Plateau. Loth et al.(1993) investigated the sensitivity of their multi-layer snow model to the value of the snow-rain criterion and found that the sensitivity is obvious. (3) In the strict sense, it is unsuitable to treat the February initial snow over the Plateau as new snow with a small density in BATS. All the above shortcomings may produce some uncertainties in the simulation results and should be improved in further studies.

Acknowledgments. This work was supported by the National Natural Science foundation of China (Grant No. 40375027) and opening item of the Key Laboratory for Meteorological Disasters and Environmental Change of Nanjing Institute of Meteorology (No. K2107).

REFERENCES

Barnett, T. P., L. Dumenil, U. Schlese, E. Roeckner, and M. Latif, 1989: The effect of Eurasian snow cover over regional and global climate variations. *J. Atmos. Sci.*, **46**, 661–685.

Chen Lieting, 2001: The role of the anomalous snow cover over the Qinghai-Xizang Plateau and ENSO in the great floods of 1998 in the Changjiang River valley. *Chinese Journal of Atmospheric Sciences*, **25**(2), 184–192. (in Chinese)

Chen Lieting, and Yan Zhixin, 1978: Influence of snow cover over the Tibetan Plateau in winter and spring on general circulation and precipitation in flood period of southern China. *Collected Papers on the Long-range Hydrological and Meteorlogical Forecast by Yangtze River Office*, Hydrological-Electrical Press, Beijing, 185–194.

Dickson, R. R., 1984: Eurasian snow cover versus Indian monsoon rainfall—An extension of the Hahn-Shukla results. *J. Climate Appl. Meteor.*, **23**, 171–173.

Dickinson, R. E., A. Henderson-Sellers, and P. J. Kennedy, 1993: Biosphere-Atmosphere Transfer Scheme(BATS) version 1e as coupled to the NCAR Community Climate Model. Tech. Note NCAR/TN-387+STR. National Center for Atmosphere Research, Boulder, CO, 72pp.

Giorgi, F., M. R. Marinucci, and G. T. Bates, 1993: Development of a second-generation regional climate model(RegCM2), Part I: Boundary-layer and radiative processes. *Mon. Wea. Rev.*, **121**, 2794–2813.

Guo Qiyun, and Wang Jiqin, 1986: The snow cover on Tibetan Plateau and its effect on the monsoon over East Asia. *Plateau Meteorology*, **5**(2), 116–124. (in Chinese)

Hahn, D. G., and S. Manabe, 1975: The role of mountains in the South Asian monsoon circulation. *J. Atmos. Sci.*, **32**, 1515–1541.

Hahn, D. G., and J. Shukla, 1976: An apparent relationship between Eurasian snow cover and India monsoon rainfall. *J. Atmos. Sci.*, **33**, 2461–2462.

Krishnamurti, T. N., 1985: Summer monsoon experiment —A review. *Mon. Wea. Rev.*, **113**, 1590–1626.

Li Peiji, 1995: Comments on "An apparent relationship between Himalayan snow cover and summer monsoon rainfall over India". *Acta Meteorologica Sinica*, **9**(3), 360–367.

Li Peiji, 1996: Discussion on the forcing of snow cover on the Qinghai-Xizang Plateau in simulation of Asian monsoon climate. *Plateau Meteorology*, **15**(3), 350–355. (in Chinese)

Liu Huaqiang, and Qian Yongfu, 2001: Effects of envelope orography and gravity wave drag parameterization on regional climate simulations. *Chinese J. Atmos. Sci.*, **25**(1), 72–84.

Loth, B., H. F. Graf, and J. M. Oberhuber, 1993: Snow cover model for global climate simulations. *J. Geophys. Res.*, **98**, 10451–10464.

Lu Xianchi, and Luo Yong, 1994: Numerical experiments on the effects of Qinghai-Xizang Plateau snow cover in winter and spring on general circulation over East Asia in summer. *Quarterly Journal of Applied Meteorology*, **5**(4), 385–393. (in Chinese)

Ose, T., 1996: The comparison of the simulated response to the regional snow mass anomalies over Tibet, Eastern Europe, and Siberia. *J. Meteor. Soc. Japan*, **74**, 845–866.

Parthasarathy, B., and S. Yang, 1995: Relationship between regional Indian summer monsoon precipitation and Eurasian snow cover. *Adv. Atmos. Sci.*, **12**, 143–150.

Qian, Y. F., Y. Q. Zheng, Y. Zhang, and M. Q. Miao, 2003: Responses of China's summer monsoon climate to snow anomaly over the Tibetan Plateau. *International Journal of Climatology*, **23**, 593–613.

Shukla, J., 1987: Interannual variability of monsoons. *Monsoons*, Fein and Stephens, Eds., A. Wiley-Interscience, 399–464.

Sun Shufen, Jin Jiming, and Wu Guoxiong, 1999: A snow model design for coupling with GCM. *Acta Meteorologica Sinica*, **57**(3), 293–300. (in Chinese)

Soman, M. K., and K. Krishna Kumar, 1993: Space-time evolution of meteorological features associated with the onset of Indian summer monsoon. *Mon. Wea. Rev.*, **121**, 1177–1194.

Vernekar, A. D., J. Zhou, and J. Shukla, 1995: The effect of Eurasian snow cover on the Indian monsoon. *J. Climate*, **8**, 248–266.

Wu Guoxiong, and Zhang Yongsheng, 1998: Thermal and mechanical forcing of the Tibetan Plateau and the Asian monsoon onset. Part I: Situating of the onset. *Scientia Atmospherica Sinica*, **22**(6), 825–838. (in Chinese)

Wu Tongwen, and Qian Zhengan, 2000: Further analyses of the linkage between winter and spring snow depth anomaly over Qinghai-Xizang Plateau and summer rainfall of eastern China. *Acta Meteorologica Sinica*, **58**(5), 570–581. (in Chinese)

Yang, Z.-L., and R. E. Dickinson, 1997: Validation of the snow submodel of the Biosphere-Atmosphere Transfer Scheme with Russian snow cover and meteorological observation data. *J. Climate*, **10**, 353–373.

Yasunari, T., A. Kitoh, and T. Tokioka, 1991: Local and remote responses to excessive snow mass over Eurasia appearing in the northern spring and summer climate–A study with the MRI-GCM-1. *J. Meteor. Soc. Japan*, **69**, 473–487.

Yasunari, T., A. Kanehira, and T. Koike, 2000: Interannual variability of snowcover over the Tibetan Plateau and its impact on Asian summer monsoon. *Proc. Conf. & Young Scientist Workshop on Asian Monsoon Environmental System and Global Change* (*AMESG*), November 15–17, Nanjing, China.

Yeh, T.-C., R. T. Wetherald, and S. Manabe, 1983: A model study of the short-term climatic and hydrologic effects of sudden snow removal. *Mon. Wea. Rev.*, **111**, 1013–1024.

Zhang Shunli, and Tao Shiyan, 2001: Influences of snow cover over the Tibetan Plateau on Asian summer monsoon. *Chinese Journal of Atmospheric Sciences*, **25**(3), 372–390. (in Chinese)

Zwiers, F. W., 1993: Simulation of the Asian summer monsoon with CCC GCM-1. *J. Climate*, **6**, 470–483.